Original Research

Identification of potential lipid biomarkers for active pulmonary tuberculosis using ultra-high-performance liquid chromatography-tandem mass spectrometry

Yu-Shuai Han[1], Jia-Xi Chen[1], Zhi-Bin Li[1], Jing Chen[1], Wen-Jing Yi[1,2], Huai Huang[1,2], Li-Liang Wei[3], Ting-Ting Jiang[2] and Ji-Cheng Li[1]

[1]Institute of Cell Biology and Department of Cardiology of the Second Affiliated Hospital, Zhejiang University School of Medicine, Hangzhou 310058, China; [2]Central Laboratory, Yangjiang People's Hospital, Yangjiang 529500, China; [3]Department of Pneumology, Shaoxing Municipal Hospital, Shaoxing 312000, China
Corresponding author: Ji-Cheng Li. Email: lijichen@zju.edu.cn

Impact statement

Tuberculosis (TB) is a serious public hygiene problem. The diagnosis of TB mainly depends on the etiological evidence, and only 51% of TB cases can be confirmed by bacteriology, which indicates that it is still difficult to diagnose TB in time based on the bacteriological detection methods. Lipid substances are closely related to the pathological processes of TB. Therefore, we used the ultra-high-performance liquid chromatography-tandem mass spectrometry technology to evaluate the changes of plasma lipid levels in TB patients. The results showed abnormal changes in the phospholipid and cholesterol ester levels. We identified phosphatidylcholine (PC, 12:0/22:2), PC (16:0/18:2), cholesteryl ester (20:3), and sphingomyelin (d18:0/18:1) as potential biomarkers in TB diagnosis. This research was devoted to exploring potential lipid biomarkers to assist in the clinical diagnosis of TB and provided clues to understand the pathogenesis of TB.

Abstract

Early diagnosis of active pulmonary tuberculosis (TB) is the key to controlling the disease. Host lipids are nutrient sources for the metabolism of *Mycobacterium tuberculosis*. In this research work, we used ultra-high-performance liquid chromatography-tandem mass spectrometry to screen plasma lipids in TB patients, lung cancer patients, community-acquired pneumonia patients, and normal healthy controls. Principal component analysis, orthogonal partial least squares discriminant analysis, and K-means clustering algorithm analysis were used to identify lipids with differential abundance. A total of 22 differential lipids were filtered out among all subjects. The plasma phospholipid levels were decreased, while the cholesterol ester levels were increased in patients with TB. We speculate that the infection of *M. tuberculosis* may regulate the lipid metabolism of TB patients and may promote host-assisted bacterial degradation of phospholipids and accumulation of cholesterol esters. This may be related to the formation of lung cavities with caseous necrosis. The results of receiver operating characteristic curve analysis revealed four lipids such as phosphatidylcholine (PC, 12:0/22:2), PC (16:0/18:2), cholesteryl ester (20:3), and sphingomyelin (d18:0/18:1) as potential biomarkers for early diagnosis of TB. The diagnostic model was fitted by using logistic regression analysis and combining the above four lipids with a sensitivity of 92.9%, a specificity of 82.4%, and the area under the curve (AUC) value of 0.934 (95% CI 0.873 – 0.971). The machine learning method (10-fold cross-validation) demonstrated that the model had good accuracy (0.908 AUC, 85.3% sensitivity, and 85.9% specificity). The lipids identified in this study may serve as novel biomarkers in TB diagnosis. Our research may pave the foundation for understanding the pathogenesis of TB.

Keywords: Pulmonary tuberculosis, plasma, lipidomics, potential biomarkers, phospholipids, cholesterol esters

***Experimental Biology and Medicine* 2021; 246: 387–399. DOI: 10.1177/1535370220968058**

Introduction

Tuberculosis (TB) is a significant public hygiene problem all over the world. About 1/4 of the world's population is infected with *Mycobacterium tuberculosis*.[1] The severity of this disease lies in the fact that a single infectious agent of *M. tuberculosis* can cause one of the highest mortality among all infectious diseases. TB is among the top 10 causes of disease-related deaths in the world. The number of new TB cases in the world continues to increase (10 million in 2018), and the TB-related mortality was also not optimistic (1.24 million in 2018).[1] TB is an infectious disease that usually attacks the lung tissue. The World Health Organization report pointed out that the percentage

of bacteriologically confirmed TB cases was only 51% of the total TB population.[1] So timely diagnosis of TB is still a perplexing clinical entity, which is of great significance for the prevention and treatment of TB.

The main pathological features of TB include the transformation of foamy macrophages, the formation of granulomas, and the formation of pulmonary cavities with caseous necrosis.[2,3] The cell wall of *M. tuberculosis* is enriched in lipids such as lipoarabinomannan and trehalosedimycolate that can stimulate CD4+ T cells to secrete interferon-gamma (IFN-γ)[4] and may invoke the host immune response to form foam cells (macrophages). The whole-genome microarray analysis of *M. tuberculosis* revealed that lipopolysaccharides and lipid metabolism genes were highly expressed in caseous TB granulomas.[5] Moreover, several studies have disclosed the accumulation of abundant cholesterol esters (CE) and triglycerides (TG) in the lipid droplets of foam cells.[4,6] When the intracellular environmental nutrition is inadequate, *M. tuberculosis* can secrete lipolytic enzymes to synthesize new lipids.[7]

It has been demonstrated that the lipid status of the host is closely related to the pathogenesis of *M. tuberculosis*. However, the lipid metabolism in the plasma of the host infected with *M. tuberculosis* has not been fully elucidated. Our previous work has revealed that miR-423-5p was involved in the cholesterol metabolism,[8] and serum amyloid A may play a significant role in the lipid metabolism.[9] We also found by utilizing the untargeted metabolomics analysis on plasma from pulmonary TB patients that the arachidonic acid lipid level was normalized after the completion of anti-TB treatment,[10] but the types of lipids identified by the untargeted technology were limited. Therefore, in the present study, we used the ultra-high-performance liquid chromatography-tandem mass spectrometry (UPLC-MS/MS) technology to screen differentially expressed plasma lipid metabolites in TB patients and in patients with other lung diseases in order to evaluate the performance of lipid metabolites as potential biomarkers to assist in diagnosing TB in time. Our research may add novel insights into the biological functions as well as the pathogenesis of the disease.

Materials and methods

Study participants

The research cases were recruited from the Enze Medical Center (China), Shaoxing Municipal Hospital (China), Zhejiang Cancer Hospital (China), and Zhejiang People's Hospital (China) between March 2017 and August 2019. The plasma samples anticoagulated with Ethylene Diamine Tetraacetic Acid (EDTA) were obtained from 34 TB patients, 30 normal healthy controls (NC), 25 lung cancer (LC) patients, and 30 community-acquired pneumonia (CAP) patients (Table 1).

The diagnostic criteria for TB (WS 288 – 2017) issued by the National Health Council of the People's Republic of China were our standard for the inclusion of TB patients into the research cohort: (1) sputum acid fast bacilli staining smear positive under the microscope or *M. tuberculosis* culture positive with chest radiographic manifestations of TB; (2) positive *M. tuberculosis* nucleic acid test with chest radiographic manifestations of TB; (3) pathological changes of TB in pulmonary tissue specimens; and (4) clinically diagnosed cases of TB responding to anti-TB treatment. And all patients in the TB group were not infected with HIV.

The diagnostic criteria for CAP patients were based on the guidelines for the diagnosis and treatment of adult CAP in China. The diagnostic criteria include (1) infectious pulmonary parenchymal inflammation acquired outside the hospital, including pneumonia that developed during the incubation period after exposure to a pathogen with a clear latency period; and (2) clinical manifestations associated with pneumonia but exclusive for TB, LC, non-infectious interstitial lung disease, pulmonary edema, atelectasis, pulmonary embolism, pulmonary eosinophil infiltration, and pulmonary vasculitis. LC patient's inclusion criteria were as follows: All LC cases were diagnosed by histopathology and immunohistochemistry. The subjects in the NC group were healthy individuals.

UPLC-MS/MS lipidomics detection

Sample extraction. The plasma samples were removed from –80°C refrigerator and thawed in a centrifuge tube. After thawing, the plasma samples were swirled and mixed for 10 s and then centrifuged for 5 min (centrifugation velocity: 3000 rpm, temperature: 4°C). Then, 50 μL of the sample was added to the corresponding centrifuge tube, and 1 mL of lipid extraction solution (including the internal standard mixture) was added, followed by vortexing for 2 min, sonication for 5 min, and the addition of 500 μL water. Afterwards, the sample was then vortexed again for 1 min and centrifuged for 10 min (centrifugation velocity: 12,000 rpm, temperature: 4°C). After centrifugation, 500 μL of the supernatant was aspirated into a centrifuge tube and concentrated. Then, the sample was reconstituted with 100 μL of mobile phase B and injected into chromatography and mass spectrometry systems for detection.

Conditions of chromatographic collection. UPLC was used to separate metabolites in plasma samples and collect chromatographic information (Shim-pack UFLC SHIMADZU CBM A system, https://www.shimadzu.com/). Thermo C30 column (2.6 μm, 2.1 mm × 100 mm) was performed as the separation system. The mobile phase A was 60% acetonitrile aqueous solution, and the mobile phase B was 10% acetonitrile isopropanol solution separately. In addition, both mobile phases contained 0.04% acetic acid and 5 mmol/L ammonium formate. The elution gradient was set in compliance with the following ratio and time point: 0 min, 20% B; 3 min, 50% B; 9 min, 75% B; 15.5 min, 90% B. The column temperature was set at 45°C, and 2 μL was injected at a flow rate of 350 μL/min.

Conditions of tandem mass spectrometry. MS/MS was used to collect the information of ion chromatographic peaks from UPLC (QTRAP®, https://sciex.com/). Electrospray ionization temperature was set at 550°C. The

Table 1. Baseline characteristics of the study population.

					P value			
Characteristics	**TB ($n = 34$)[c]**	**LC ($n = 25$)[c]**	**CAP ($n = 30$)[c]**	**NC ($n = 30$)[c]**	**NC vs. TB[a]**	**LC vs. TB[a]**	**CAP vs. TB[a]**	**All groups[b]**
Age, years (mean)	41.6 ± 14.8	49.7 ± 11.2	44.2 ± 15.5	43.4 ± 12.1	0.558	0.039	0.443	0.132
Sex (female)	13 (38.2%)	13 (52.0%)	18 (60.0%)	13 (43.3%)	0.679	0.293	0.082	0.327
BMI (kg^2/m)	21.1 ± 2.9	23.2 ± 2.8	22.5 ± 3.6	21.9 ± 2.4	0.444	0.065	0.341	0.347
TG (mmol/L)	0.99 ± 0.34	1.25 ± 0.64	1.23 ± 1.23	0.96 ± 0.34	0.730	0.094	0.988	0.295
CHOL (mmol/L)	4.32 ± 0.83	4.57 ± 0.93	3.87 ± 0.76	4.57 ± 0.68	0.324	0.947	0.037	0.006
HDL (mmol/L)	1.17 ± 0.37	1.23 ± 0.31	1.07 ± 0.26	1.30 ± 0.21	0.064	0.164	0.428	0.022
LDL (mmol/L)	2.5 ± 0.67	2.88 ± 0.72	2.31 ± 0.69	2.83 ± 0.53	0.088	0.103	0.260	0.011
CT (caseous necrosis cavity) (+/–)	14/20	NA	NA	NA	NA	NA	NA	NA
Sputum bacteria (+/–)	28/6	NA	NA	NA	NA	NA	NA	NA
Bronchial tuberculosis (+/–/NA)	7/23/4	NA	NA	NA	NA	NA	NA	NA
Pleural effusion (+/–)	3/31	NA	NA	NA	NA	NA	NA	NA

TB: tuberculosis; LC: lung cancer; CAP: community-acquired pneumonia; NC: normal healthy controls; BMI: body mass index; TG: triglycerides; HDL: high-density lipoprotein; LDL: low-density lipoprotein; CT: computed tomography; NA: not available.
[a]Kruskal–Wallis test.
[b]Mann–Whitney U test (continuous variables), Chi-square test (categorical variables).
[c]Data are mean ± SD for the continuous variables, number (%) for categorical variables.

mass spectrum voltage was 5500 V; the ion source gas I (GSI), the gas II (GSII), and the curtain gas (CUR) were set at 55, 60, and 25 psi, respectively. The parameter of collision-activated dissociation was set at medium. Each ion pair was scanned according to the optimized declustering potential and collision energy . There was positive and negative ion mode under the scans of Linear Ion Trap (LIT) and triple quadrupole (QQQ). The whole scanning process was controlled by analyst 1.6.3 software (SCIEX).

Qualitative and quantitative analysis of lipidomics data

The metabolites in the samples were analyzed qualitatively and quantitatively according to the internal metabolite database. The signal intensity of the characteristic ions in counts per second was obtained in the detector, and the chromatographic peaks were integrated and corrected using MultiQuant. The relative abundance of lipid metabolites in plasma was obtained by calculating the peak area of each chromatogram in mass spectrometry data. The analytical processing of raw data was completed in the software Analyst 1.6.3.

Statistical analysis

The baseline characteristics of the study population were statistically analyzed by Chi-square test, Kruskal–Wallis H test, and Mann–Whitney U test. P value <0.05 indicated statistical significance. Firstly, the data quality of lipid metabolites in terms of homogeneity and reproducibility was evaluated by the principal component analysis (PCA). And then, the orthogonal partial least squares discriminant analysis (OPLS-DA) method was applied to remove irrelevant variables. Meanwhile, the variable importance in the projection (VIP) values were obtained from each lipid variable to measure the contribution of variables to the model. The quality of the OPLS-DA was validated by the permutation test. The t-test was used to obtain P values of each individual variables, followed by the adjustment of false discovery rate (FDR) by multiple hypothesis tests. The above results were acquired by R 3.5.3. The differentially expressed lipid metabolites were determined by a combination of fold change (FC), FDR, and VIP values. The area under the curve (AUC), sensitivity, and specificity of 22 differentially expressed lipids in the TB group and the other groups were obtained by the receiver operating characteristic (ROC) curve (SPSS 25.0). The logistic regression analysis was performed to evaluate the diagnostic value of the combined biomarkers model (MedCalc 19.0.7). The 10-fold cross-validation method was used to verify the accuracy of our diagnostic model (MetaboAnalyst 4.0).

Bioinformatics analysis

Patients in the TB group were further divided into two subgroups, the TB-N subgroup (patients with lung cavities) and the TB-P subgroup (patients without lung cavities) based on the chest computed tomography (CT) imaging findings. The changes in lipids between the NC group and TB subgroups were evaluated by utilizing K-means clustering algorithm, and the K value was assigned to 6. The multivariate polyline trend graph was drawn by GraphPad prism 8.0.2. The analysis of metabolic pathways was performed by the Kyoto Encyclopedia of Genes and Genomes (KEGG) (https://www.kegg.jp/). The enrichment of differential expression lipids in different disease groups was visualized. The Pearson correlation coefficients of differentially expressed lipid metabolites (NC vs. TB) and candidate potential biomarkers were analyzed using software SPSS 25.0. The differentially expressed lipid metabolites correlation network was visualized by Cytoscape 3.7.2.

Results

Baseline characteristics of the study population

The clinical characteristics of the study population were described in Table 1. The chest CT imaging findings in the

study population revealed that 14 out of 34 patients in the TB group had lung cavities with caseous necrosis, which was the main reason to divide the TB group into two subgroups.

Patients in the LC group were older than the patients in the TB group ($P = 0.039$), which was related to the epidemiological characteristics of TB[1,2] and LC.[11] The total cholesterol level in the CAP group was lower compared to the TB group ($P = 0.037$) and the other groups, indicating an elevated consumption of cholesterol in acute pulmonary infection (pneumonia). Although the results of biochemical tests were within the normal range in CAP patients, they were at the lower end of the standard range.

Results of lipidomics experiments

In this study, 119 plasma samples from the four groups were screened by using UPLC-MS/MS, and the samples were qualitatively and quantitatively categorized into 20 types, including 425 differential lipid metabolites (81 differential lipids in negative and 324 in positive peaks). The qualitative data showed that the positive and negative total ionization chromatography had good results (Supplementary Figures 1 and 2). The scatter diagram of PCA illustrated the quality control process on experimental data. The green scatter points representing mixed samples were highly aggregated in the graph, indicating that the detection process was stable (Supplementary Figure 3). The data of plasma lipids in the four groups (TB, LC, CAP, and NC groups) were analyzed by using the OPLS-DA method. According to the characteristics of the model, the data of any two groups could be well distinguished (Figure 1(a), (c), and (e)), and the VIP value for each lipid was calculated (Supplementary Tables 1 to 3). The higher the VIP value, the more the contribution of the substance to the model construction. The verification results of the 200 random permutations and combination verification model data showed $P < 0.005$, indicating that the OPLS-DA model was not over-fitting and was reliable to screen lipid biomarkers (Figure 1(b), (d), and (f)).

The differentially expressed lipid metabolites were determined based on the following criteria: (1) FC >1.2 or <0.83, (2) VIP ≥ 1.0, and (3) FDR value <0.05 (Supplementary Tables 1 to 3). Between the NC and the TB groups, a total of 120 differentially expressed lipids were identified (62 down-regulated and 58 up-regulated lipids) (Supplementary Figure4(a)); between the LC and the TB groups, a total of 60 differentially expressed lipids were identified (37 down-regulated and 23 up-regulated lipids) (Supplementary Figure4(b)); and between the CAP and the TB groups, a total of 92 differentially expressed lipids were identified (78 down-regulated and 14 up-regulated lipids) (Supplementary Figure4(c)).

Analysis of lipids in pulmonary TB

Our data described the characteristics of plasma lipid metabolism in patients with pulmonary TB. Compared with the NC group, the TB group had different categories and quantities of plasma lipids, which were shown in the volcano chart (Figure 2(a)). The differentially expressed lipids were mainly members of the phosphatidylcholine (PC), CE, lysophosphatidylcholine, diglyceride (DG), sphingomyelin (SM), and TG. The K-means clustering analysis further revealed 120 differentially expressed lipid metabolites between the NC group and the TB group, and there was a changing trend in the NC group, the TB-N subgroup, and the TB-P subgroup. The minimum distance between the clusters was 0.745. The clustering algorithm was achieved by 6 iterative calculation steps, and the K value was assigned to 6 (Figure 2(b) to (g)). The pattern of Clusters 3, 4, and 6 showed a significant upward or downward trend. The metabolites in each cluster were listed in Table 2. Among the substances in Cluster 3 (Figure 2(c)), 17 differentially expressed lipid metabolites were decreased in the TB-N subgroup in comparison with the NC group, and the down-regulation was augmented in the TB-P subgroup. These substances were mainly phospholipids, including PC, lysophosphatidylethanolamine, and SM. Cluster 4 (Figure 2(d)) showed a similar trend as Cluster 3, but the downward trend was less steep. PC was also the predominant component of Cluster 4 (Table 2). The results of Cluster 3 and Cluster 4 suggested that the levels of plasma phospholipids were down-regulated in TB patients, which was more obvious in the patients with lung cavities. Another characteristic cluster was Cluster 6 (Figure 2(e)), which exhibited the opposite trend to Cluster 3 and Cluster 4. The 23 substances in Cluster 6 were increased in the TB-N subgroup in comparison with the NC group, and the concentration of these metabolites was even higher in the TB-P subgroup. Most of the substances in Cluster 6 were CEs and glycerides. These three clusters highlighted the potential mechanisms of plasma lipids in the pathogenesis of TB.

Lipids differentiating TB from CAP and LC

A significant difference in plasma lipid profiles of the TB group was observed by comparison with the CAP group. As CAP and TB both are infectious diseases of the lungs, the phospholipids were consistently down-regulated in these two groups, but the downward trend was more significant in the TB group. The trend of TG was similar between the two groups. High-unsaturated (more than six double bonds) TG showed a downward trend, while low-unsaturated TG showed an upward trend. In addition, CEs in the CAP group exhibited a more conspicuous downward trend by comparison with the TB group. Besides, the KEGG pathway analysis showed that the abnormalities of lipid metabolism in the TB group were characterized by the altered phospholipid metabolism and fatty acid metabolism (Figure 3(a) and (b)), which may be related to *M. tuberculosis* reproduction and degradation of membrane phospholipids. The lipid metabolic abnormalities of the CAP group were characterized by the lipid metabolism signaling pathway and fatty acid chain elongation and degradation (Supplementary Figure 5(a)). The levels of plasma TG were significantly up-regulated, while the levels of plasma free fatty acid (FFA) were conspicuously decreased in the LC group, unlike the patterns of these substances in the TB and CAP groups. The differentially expressed lipids

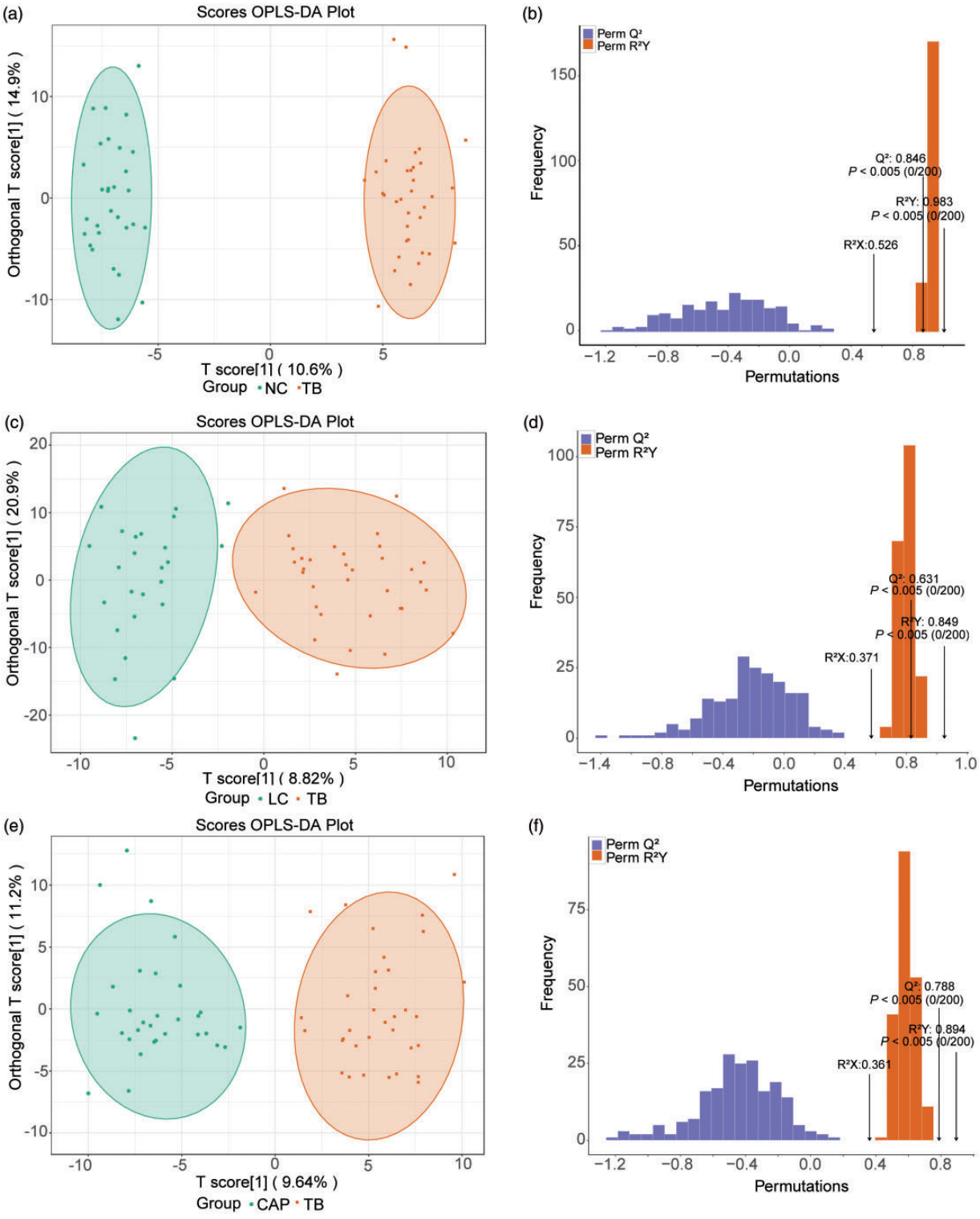

Figure 1. The multivariate statistical model of the TB, NC, LC, and CAP groups. Scatter plot of OPLS-DA model and validation model of permutation test: (a, b) NC vs. TB: $R^2X = 0.526$, $R^2Y = 0.983$, $Q^2 = 0.846$, $P < 0.005$. (c, d) LC vs. TB: $R^2X = 0.371$, $R^2Y = 0.849$, $Q2 = 0.631$, $P < 0.005$. (e, f) CAP vs. TB: $R^2X = 0.361$, $R^2Y = 0.894$, $Q^2 = 0.788$, $P < 0.005$. During 200 random permutations in each group, $P < 0.005$ showed that no random matrix model had better interpretation rate of the Y matrix than the former OPLS-DA model. The model could effectively distinguish the features of two groups. (A color version of this figure is available in the online journal.)
OPLS-DA: partial least squares discriminant analysis; NC: normal healthy controls; TB: tuberculosis; LC: lung cancer; CAP: community-acquired pneumonia.

mainly had functions of fatty acid elongation, fatty acid degradation, and thermogenesis (Supplementary Figure 5 (b)). We found that there existed differential characteristics of lipid metabolism in different pulmonary diseases. The characteristics of the TB group were abnormal metabolism of phospholipids and CEs, which were considered to be related to the destruction of foam cells membrane and the accumulation of lipids in caseous necrosis. PC, SM, and CE

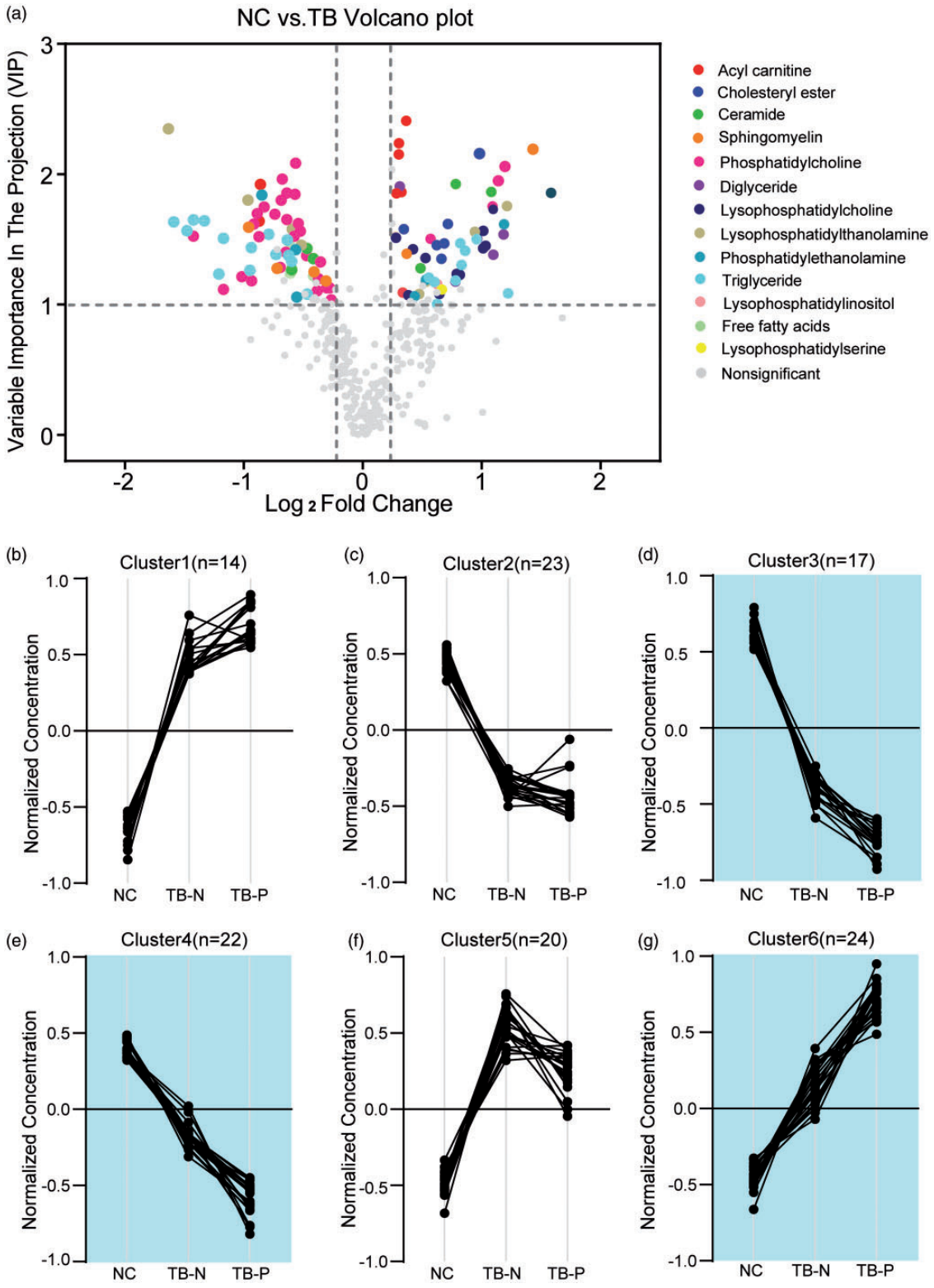

Figure 2. Volcano map and K-means clusters of differential lipids. (a) Volcano map of differential lipids classification of the TB group and the NC group. The abscissa is an FC; the ordinate is the VIP obtained based on OPLS-DA model. Lipids with *P* value obtained by *t*-test and FDR <0.05 verified by multiple hypothesis test were identified as significantly differential metabolites. Colored plots indicate upward trend and downward trend of substances, and gray plots indicate that they are not statistically significant. The line chart shows the clusters of 120 differential lipids in the TB group and the NC group after K-means clustering. The ordinate is the normalized lipid concentration. The abscissa is the NC group, the TB-N (patients without lung cavities) subgroup, and the TB-P (patients without lung cavities) subgroup. (d, e) Clusters 3 and 4 had a downward trend in the NC group, and in TB-N and TB-P subgroups. (g) Cluster 6 had upward trend in the NC group, and in TB-N and TB-P subgroups. (b, c, f) The trend of Clusters 1, 2, and 5 was non-significant. (A color version of this figure is available in the online journal.)
NC: normal healthy controls; TB: tuberculosis.

Table 2. Plasma lipids identified as changing significantly over the progression of TB.

Cluster	Lipid class	Lipids identified as changing during the progression of active pulmonary tuberculosis
Cluster 3	Phosphatidylcholine	PC(16:0/18:2),PC(16:1/18:2), PC(16:0/22:6), PC(14:0/18:2), PC(12:0/22:2), PC(18:1/22:6), PC(O-16:2/18:1), PC(O-18:3/20:3), PC(O-20:3/20:4), PE(P-18:2/20:4)
	Acyl carnitine	Linoleyl-carnitine
	Lysophosphatidylethanolamine	LPE(0:0/22:4), LPE(0:0/24:6)
	Phosphatidylethanolamine	PE(P-18:2/20:4)
	Sphingomyelin	SM(d18:0/18:1)
	Triglyceride	TG(18:2/18:3/20:3), TG(14:0/20:2/22:6)
Cluster 4	Free fatty acid	FFA(22:6)
	Phosphatidylcholine	PC(18:1/18:2), PC(18:2/18:2), PC(18:0/18:2), PC(14:0/18:3), PC(14:0/20:4), PC(14:0/22:6), PC(16:1/22:6), PC(18:2/22:6), PC(O-16:0/18:2), PC(O-20:2/22:1), PC(O-20:3/20:3)
	Acyl carnitine	Decenoyl-carnitine
	Ceramide	Cer(t18:0/24:0)
	Diglyceride	DG(18:2/18:2/0:0)
	Phosphatidylethanolamine	PE(P-18:2/20:1), PE(P-18:2/20:3)
	Sphingomyelin	SM(d18:2/16:1), SM(d18:2/20:1)
	Triglyceride	TG(18:2/18:2/18:2), TG(14:0/18:2/22:6)
Cluster 6	Phosphatidylcholine	PC(16:0/20:3)
	Cholesteryl ester	CE(16:1), CE(22:5), CE(20:3)
	Ceramide	Cer(d18:1/16:0), Cer(d18:1/18:0), Cer(d18:1/20:0)
	Diglyceride	DG(16:0/18:1/0:0), DG(18:0/18:1/0:0), DG(16:0/20:4/0:0)
	Lysophosphatidylcholine	LPC(O-14:0/0:0)
	Phosphatidylethanolamine	PE(18:1/18:0), PE(16:0/20:4)
	Sphingomyelin	SM(d18:1/18:0)
	Triglyceride	TG(18:0/18:1/18:1), TG(14:0/18:0/18:3), TG(14:0/18:0/20:4), TG(14:0/20:1/20:3), TG(14:0/16:1/20:4), TG(14:0/18:1/20:4), TG(14:0/20:1/22:4), TG(14:0/20:4/22:2), TG(14:0/20:1/20:4)

were the main components in these metabolic pathways, which were also the focus of our study in the pathogenesis of TB.

Screening and evaluation of lipid biomarkers in TB

Our study also provided potential clues for the early diagnosis of TB. The differential abundance and the clustering analysis of lipid metabolites among the four groups were visualized in the heatmap (Supplementary Figure 6(a) to (c)). We identified 22 differentially expressed lipids that could distinguish TB from the other groups (NC vs. TB, LC vs. TB, and CAP vs. TB) (Figure 4(a), Supplementary Figure 6(d)). The diagnostic efficacy of 22 differentially expressed lipids was evaluated by the ROC curve between the TB patients and the other controls, and the values of AUC, FC, specificity, and sensitivity were obtained (Table 3). Among 22 differentially expressed lipids, 4 lipids such as PC (12:0/22:2), PC (16:0/18:2), CE (20:3), and SM (d18:0/18:1) were selected as potential diagnostic biomarkers for TB (Figure 4(b)). Among them, the AUC value of PC (12:0/22:2) was 0.878 with 76.5% specificity and 91.1% sensitivity (Figure 4(c)); the AUC value of PC (16:0/18:2) was 0.863 with 82.4% specificity and 82.4% sensitivity (Figure 4(f)); the AUC value of CE (20:3) was 0.863 with 83.5% specificity and 79.4% sensitivity (Figure 4(e)); and the AUC value of SM (d18:0/18:1) was 0.822 with 90.6% specificity and 73.4% sensitivity (Figure 4(d)). In order to evaluate the diagnostic capacity of the four potential markers in combination, we used the logistic regression method to obtain an integrated diagnostic model with a sensitivity of 92.3%, a specificity of 82.4%, and the AUC value of 0.934 (95% CI 0.873 – 0.971) (Figure 5(a)). Furthermore, the 10-fold cross-validation method was used to test the performance of the logistic regression model. The results illustrated that the model could discriminate TB from non-TB and NC with an AUC of 0.908 (85.3% sensitivity, 85.9% specificity) (Figure 5(b)).

Differentially expressed lipids network analysis of TB

The Pearson correlation coefficients between the candidate biomarkers and other differential lipid metabolites were calculated. The related pairs were selected if the coefficients were in the range of <-0.4 or >0.4, and a lipid network was established (Figure 6). We found that PC and SM had a positive synergistic regulatory relationship, while DGs and CEs, and phospholipids and CEs had a negative synergistic regulatory relationship. And this phenomenon also existed in sputum negative and positive TB patients.

Discussion

Recent studies on TB biomarkers, including mRNA,[12] noncoding RNA,[13,14] protein,[15] and metabonomics biomarkers,[16] explored detection of latent infection of *M. tuberculosis*,[15] early diagnosis of drug-sensitive or drug-resistant TB,[15,17] efficacy evaluation of anti-TB treatment,[10,13] and predicting the risk of recurrent TB after being cured.[18] Our study was carried out by UPLC-MS/MS technology and used in-house metabolites database to analyze lipid profiles of TB. Furthermore, the potential lipid biomarkers of TB were identified based on the results of extensive targeted-detection.

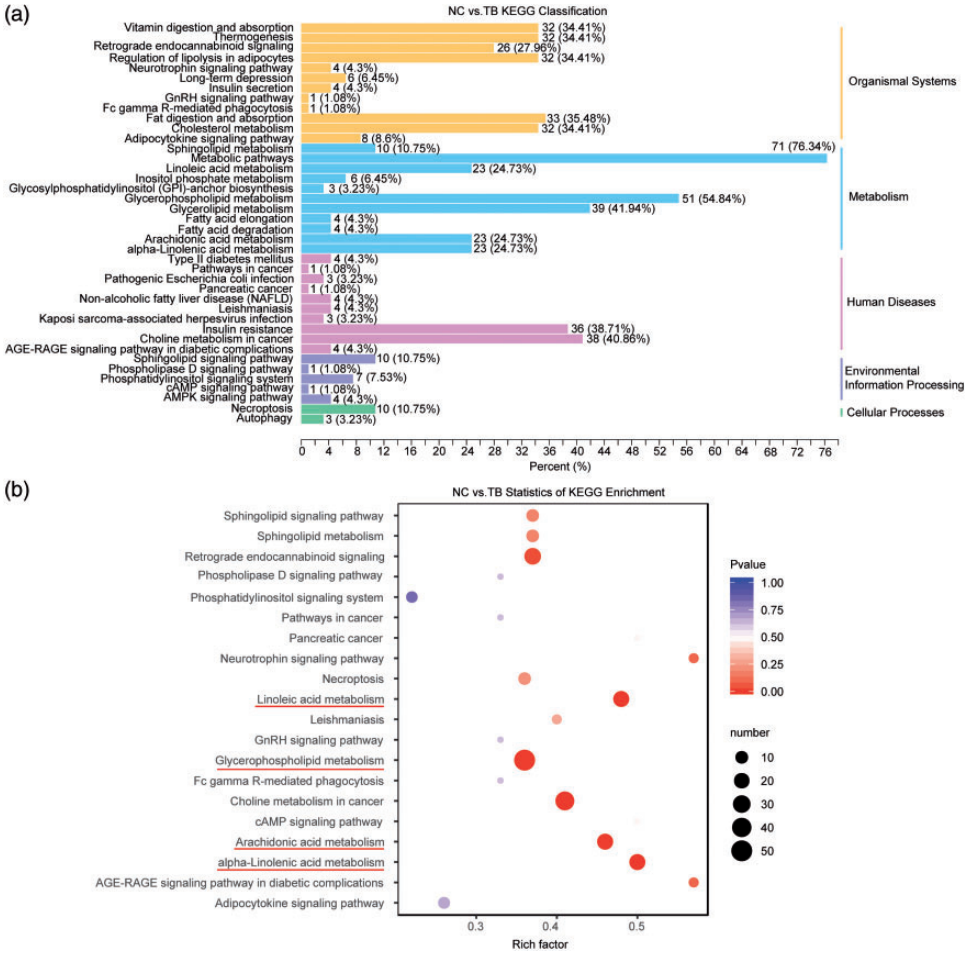

Figure 3. KEGG substance classification and enrichment analysis of differential lipids in the NC and TB groups. (a) KEGG substance classification, the left ordinate is the pathway where the lipid substance is located, the right ordinate is the classification of each metabolic pathway, and the abscissa represents the proportion of the substance in the pathway. (b) Statistics of KEGG substance enrichment. The left coordinate represents the enriched pathway, and the abscissa represents the rich factor. The results showed significant enrichment in phospholipid, linoleic acid, linolenic acid, and arachidonic acid metabolism (red underline). (A color version of this figure is available in the online journal.)

NC: normal healthy controls; TB: tuberculosis; KEGG: Kyoto Encyclopedia of Genes and Genomes; GnRH: gonadotropin-releasing hormone; AMPK: 5' adenosine monophosphate-activated protein kinase; cAMP: cyclic adenosine monophosphate; AGE-RAGE: advanced glycation end products-receptor for advanced glycation end products.

The results showed that plasma phospholipids concentration decreased in patients with TB. Phospholipids are abundant in the circulating blood and are involved in the formation of the lipid bilayer structure of the cell membrane,[19] accounting for 70–80% of the pulmonary surfactant components.[20] PC and SM were significantly down-regulated in patients with TB. The KEGG metabolic pathway illustrated that the TB group was represented by the degradation of phospholipids by phospholipases to produce FFA ($P < 0.05$). The plasma lipids may provide a carbon source for metabolism and reproduction of *M. tuberculosis*.[21] Phospholipases are closely related to phospholipid degradation and can be divided into phospholipases A1, A2, B1, B2, C, and D.[22] Studies have shown that phospholipase is of great importance contributing to the virulence of bacterial specials and has been identified and detected in various bacteria.[23] For example, the infection of *Clostridium perfringens* can give rise to gas gangrene, and the destruction of skin and lung tissue can be invaded by *Pseudomonas aeruginosa*.[23] *Toxoplasma gondii* has been demonstrated to use phospholipase to enhance the destruction and toxicity of host cells.[24] De Groote *et al*.[25] studied a large number of samples from TB patients and found that NPS-PLA2 (secreted phospholipase A2) was significantly expressed upward in serum of TB patients and had a potent capacity to diagnose TB. The free cholesterol in the host plasma can be catalyzed by the secreted phospholipase A2 to produce cholesteryl phosphatidylcholine side chain,[26] which was consistent with the trend of lipid changes in our study (Pearson correlation = –0.64). *M. tuberculosis* infection may disrupt the metabolic function of host phospholipids.[21] In addition, *M. tuberculosis* can encode RV0888 SM hydrolase, which can mediate the degradation of PC and glucose uptake[27,28] and can prevent maturation of phagosomes and inhibit autophagy,[27] indicating the role of *M. tuberculosis* in escaping phagocytic cells. SM hydrolase can also mediate the transport of bacteria from macrophages to caseous granuloma and can use host phospholipids to degrade fatty acids into energy and carbon sources[28]

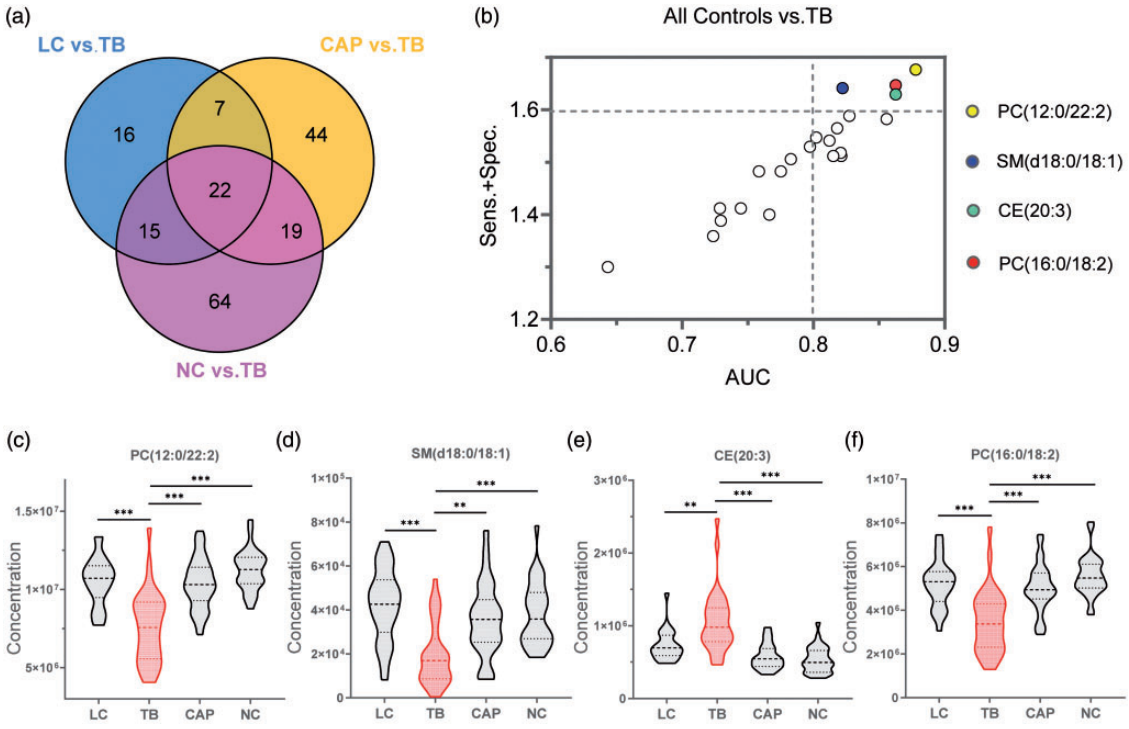

Figure 4. Screening and evaluation of potential lipid biomarkers in TB. (a) Venn diagram showing the number of differential lipids in different groups NC vs. TB, CAP vs. TB, and LC vs. TB (FC >1.2 or <0.83, VIP ≥1, and FDR <0.05). (b) The 22 differential lipids abundance were analyzed by ROC. The abscissa is the AUC value of each lipid, and the ordinate is the specificity + sensitivity value. Four colored spots indicated that the AUC value is greater than 0.8, and the specificity + sensitivity value is greater than 1.6. The violin diagram showing PC (12:0/22:2) (c), PC (16:0/18:2) (d), CE (20:3) (e), and SM (d18:0/18:1) (f) concentration. The abscissa is each component group, and the ordinate is mass spectral concentration integration data. **FDR <0.01, ***FDR <0.001. (A color version of this figure is available in the online journal.) LC: lung cancer; TB: tuberculosis; CAP: community-acquired pneumonia; NC: normal healthy controls; AUC: area under the curve; PC: phosphatidylcholine; SM: sphingomyelin; CE: cholesterol ester.

Table 3. The ROC reports between all controls compared with TB.

Compounds	AUC	*P* value[b]	Fold change	Type	Sensitivity	Specificity	Sens. + Spec.[a]
PC(12:0/22:2)	0.878	2.4505E-14	0.709	Down	0.912	0.765	1.676
PC(16:0/18:2)	0.862	1.2614E-11	0.661	Down	0.824	0.824	1.647
CE(20:3)	0.863	3.1503E-12	1.734	Up	0.794	0.835	1.629
SM(d18:0/18:1)	0.822	1.8357E-8	0.508	Down	0.735	0.906	1.641
LPC(22:2/0:0)	0.856	8.4246E-13	2.231	Up	0.735	0.847	1.582
PC(14:0/20:3)	0.827	2.271E-8	0.615	Down	0.765	0.824	1.588
LPE(0:0/18:0)	0.821	3.5475E-11	2.225	Up	0.735	0.776	1.512
LPC(O-20:1/0:0)	0.821	2.274E-11	2.108	Up	0.706	0.812	1.518
PC(14:0/18:2)	0.818	8.9375E-8	0.546	Down	0.647	0.918	1.565
LPC(20:1/0:0)	0.815	1.6449E-8	2.136	Up	0.794	0.718	1.512
CE(18:0)	0.812	1.4412E-8	1.327	Down	0.765	0.776	1.541
PC(16:1/18:2)	0.802	3.398E-7	0.601	Down	0.676	0.871	1.547
LPC(20:3/0:0)	0.797	1.0393E-9	2.440	Up	0.765	0.765	1.529
LPC(18:0/0:0)	0.783	1.9721E-10	2.118	Up	0.588	0.918	1.506
LPC(18:1/0:0)	0.775	7.8219E-8	1.461	Up	0.706	0.776	1.482
CE(22:4)	0.766	4.7717E-7	1.469	Up	0.941	0.459	1.400
Cer(d18:1/18:0)	0.758	2.5363E-6	1.693	Up	0.765	0.718	1.482
SM(d18:2/20:1)	0.745	9.2294E-5	0.577	Down	0.647	0.765	1.412
LPC(20:2/0:0)	0.729	6.8844E-7	1.608	Up	0.706	0.682	1.388
SM(d18:1/18:0)	0.729	2.4628E-6	1.290	Up	0.706	0.706	1.412
TG(14:0/16:0/22:4)	0.724	2.3357E-4	0.610	Down	0.971	0.388	1.359
Linoleyl-carnitine	0.643	0.011602	0.752	Down	0.853	0.447	1.300

AUC: area under the curve; PC: phosphatidylcholine; CE: cholesterol ester; SM: sphingomyelin; LPC: lysophosphatidylcholine; LPE: lysophosphatidylethanolamine; TG: triglyceride.
[a]Sens.: Sensitivity; Spec.: Specificity.
[b]*P* values were calculated by *t*-test.

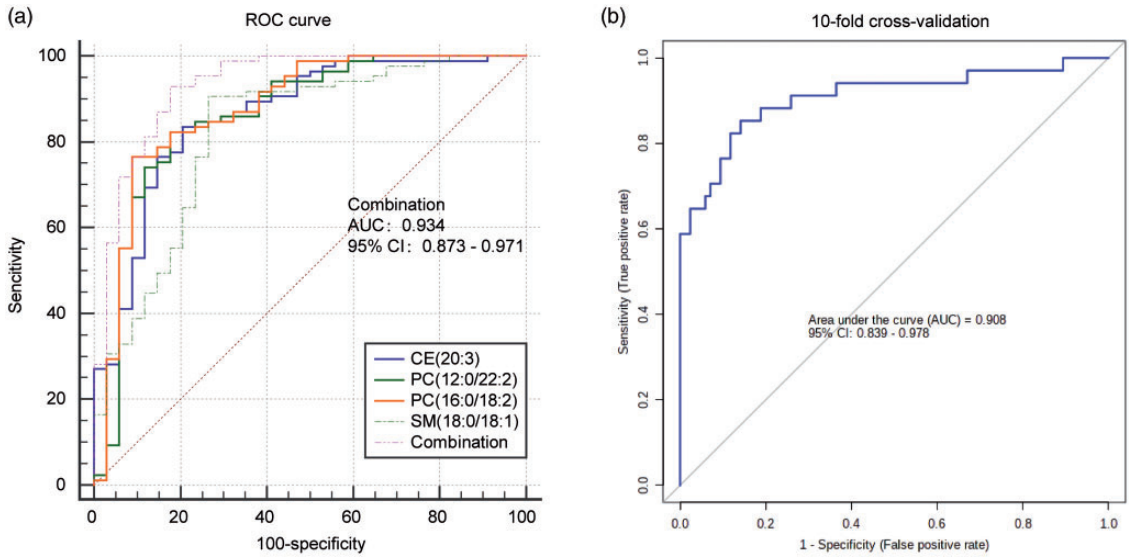

Figure 5. ROC curve diagnostic model and 10-fold cross-validation for assessing lipid biomarkers of pulmonary TB. (a) The ordinate indicates sensitivity, and the abscissa indicates specificity. CE (20:3), PC (12:0/22:2), PC (16:0/18:2), and SM (18:0/18:1) combined diagnostic model has a sensitivity of 92.9%, a specificity of 82.4%, and the AUC value of 0.934; 95% confidence interval (95% CI 0.873–0.971).(b) The data set was divided into 10 parts, 9 of which were used as training data and 1 as test data. The verification of 10-fold cross-validation revealed logistic regression model with an AUC of 0.908, 85.3% sensitivity and 85.9% specificity. (A color version of this figure is available in the online journal.)
ROC: receiver operating characteristic; AUC: area under the curve; PC: phosphatidylcholine; SM: sphingomyelin; CE: cholesterol ester

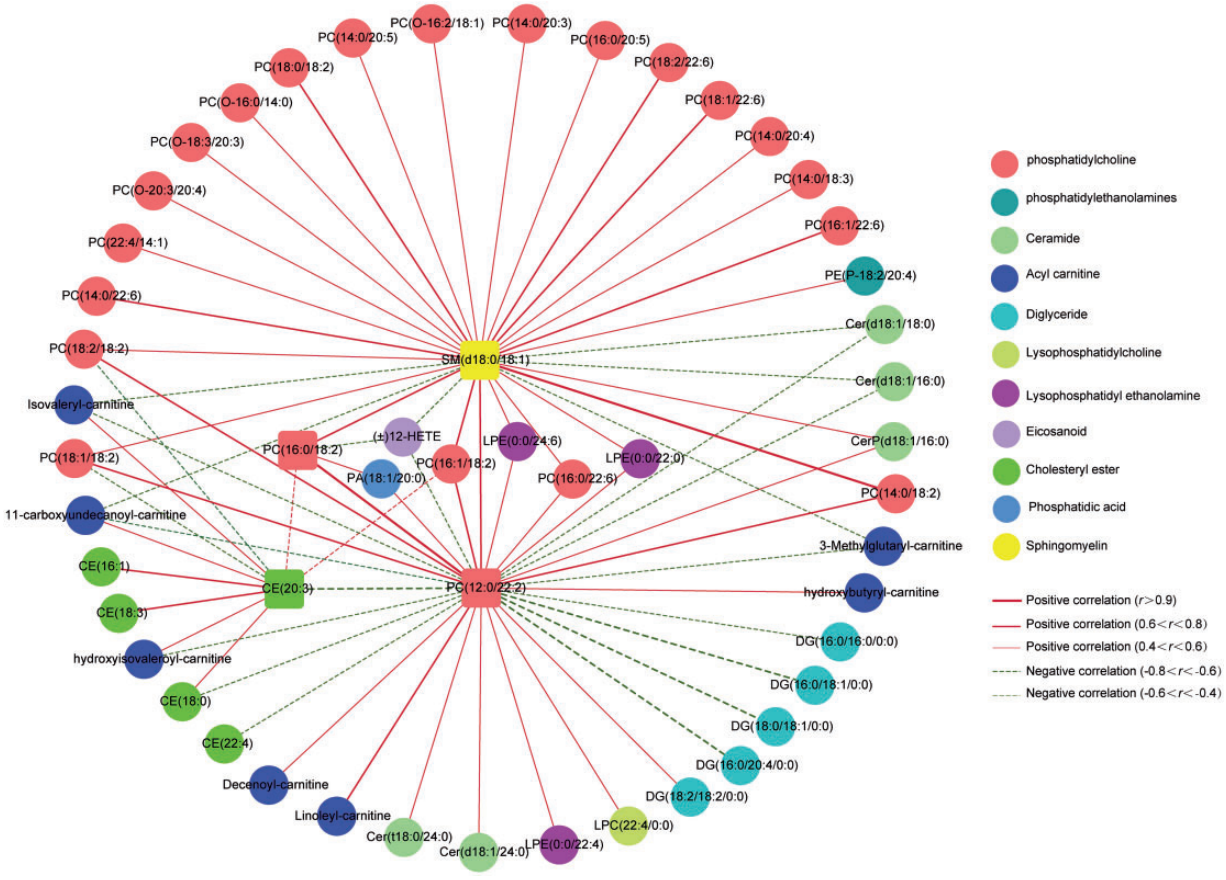

Figure 6. Differential lipids metabolism network. The network surrounding the four potential biomarkers with the best diagnostic efficacy between the NC and TB groups. The synergistic regulation relationship of various lipids in plasma was observed by using Pearson correlation coefficient. Colored circles represent different lipid classes, solid red lines indicate positive correlation between substances, and green dashed lines indicate negative correlation between substances. Correlation coefficient >0.9 or <–0.9 means pole-strength correlation, 0.6 to 0.8 or –0.8 to –0.6 means strong correlation, and 0.4 to 0.6 or –0.6 to –0.4 means moderate correlation. (A color version of this figure is available in the online journal.)
PC: phosphatidylcholine; PE: phosphatidylethanolamine; CE: cholesterol ester; SM: sphingomyelin; PA: phosphatidic acid; LPE: lysophosphatidylethanolamine; HETE: hydroxyeicosatetraenoic acid; LPC: lysophosphatidylcholine; DG: diglyceride.

to form a reproduction ecology niche, which is conducive to the spread of bacteria.

The ROC curve showed that PC (12:0/22:2), PC (16:0/18:2), and SM (d18:0/18:1) were capable of discriminating TB from non-TB. The above three lipids were positively correlated, showing a further downward trend in patients with lung cavities, as indicated by the Cluster 3 results (Figure 2(d)). The formation of lung cavities indicated caseous necrosis that can be ruptured into the airway after liquefaction and is more likely to cause the spread of *M. tuberculosis*. Interestingly, the results of this study were closely related to the degree of necrosis. Besides, some studies have demonstrated that the genome of *M. tuberculosis* has abundant genes encoding phospholipases,[29,30] suggesting that drugs can be developed to interfere with the expression of phospholipase gene to change the energy metabolism of *M. tuberculosis*[30] in order to block the destruction of host cells. However, the aforementioned enzymes are also of great abundance in the cells of the human body, and further studies are needed to find specific inhibitors for *M. tuberculosis* lipolytic enzymes.[7]

In addition, we observed an up-regulated concentration of CEs in the plasma of patients with TB. Studies have shown that lipid droplets isolated from *M. tuberculosis*-infected granulomas had abundant CEs accumulation.[31,32] And the formation of lipid droplets in immune cells can play a key role in host–pathogen interactions. The lipid droplets of the body's cells can be attacked by a variety of pathogenic microorganisms[33] and can form favorable microecological niches to assist pathogens in avoiding immune surveillance and strengthening escape.[34] It has been shown that the accumulation of CEs can activate toll-like receptor signaling, and proliferation and differentiation of inflammatory cells, such as monocytes and neutrophils, leading to an enhanced inflammatory response.[35] *M. tuberculosis* has specific enzymes and energy pathways for cholesterol metabolism.[36] In our previous study, we found that serum amyloid A was up-regulated in patients with TB,[9] which can promote the esterification of cholesterol.[37] In addition, IFN-γ is a delayed hypersensitivity protein, secreted by TH1 cells after being activated by *M. tuberculosis*. It can regulate the expression of acyl-coenzyme A and can mediate the reduction of CE efflux in foam cells.[38] Studies have shown that *M. tuberculosis* can recruit CEs and promote the host to accelerate the synthesis of CEs without degrading. This is consistent with our findings. The level of CEs of plasma was increased in patients with TB. Therefore, we speculated that the accumulation of host CEs is conducive to *M. tuberculosis* survival and reproduction, accumulating antigens, increasing immune attack, and facilitating *M. tuberculosis* spread after cellular necrosis and disintegration. Pathological examination of the tissues and imaging studies of TB lesions in this study revealed that the clogging of the alveoli by macrophages rich in CEs can provide an isolated environment for the proliferation of *M. tuberculosis* and can create conditions for tissue necrosis.[2] In clinical practice, statins (that can decrease plasma cholesterol levels and increase the resistance to *M. tuberculosis* infection) have been used to treat TB patients.[39] Therefore, blocking CE synthesis in *M. tuberculosis* may be the adjuvant therapeutic target for anti-TB medications.

Considering that the lipidomics is a highly sensitive omics methodology, we used the FDR value to filter differential biomarkers.[40] In order to observe the changes in lipids, we expanded the screening range of FC. In addition, we divided TB patients into further subgroups based on the presence of caseous necrosis (lung cavity) on the chest CT scan or not. The small sample size is the limitation of our research, and we did not evaluate the size of the inner walls of the lung cavities. However, we used 10-fold cross-validation to evaluate the performance of the diagnostic model. Therefore, in the future study, we plan to increase the number of samples to verify the value of our candidate biomarkers and to evaluate the disease condition in more detail.

In this study, we used the UPLC-MS/MS technology for the first time to study the alterations in various types of lipid metabolism in pulmonary TB with or without caseous necrosis (lung cavity). We found that the interaction between *M. tuberculosis* and host lipid metabolism can cause characteristic changes in patients with TB. The phospholipids and CEs metabolism may form niches that were conducive to the propagation and energy metabolism of *M. tuberculosis*. Interfering with the expression of phospholipid hydrolase coding gene or blocking the synthesis of CEs may be potential therapeutic perspectives for the treatment of TB. We obtained four potential biomarkers such as PC (12:0/22:2), PC (16:0/18:2), CE (20:3), and SM (d18:0/18:1) that could distinguish between TB and the other lung diseases. The logistic regression diagnostic model revealed a sensitivity of 92.9%, a specificity of 82.4%, and the AUC value of 0.934 (95% CI 0.873 – 0.971), and the results of 10-fold cross-validation demonstrated that the model could distinguish TB patients from non-TB patients and NC with good accuracy (0.908 AUC, 85.3% sensitivity, and 85.9% specificity). Our study may pave the foundation to understand the pathogenesis of TB.

AUTHORS' CONTRIBUTIONS

J-CL designed this research project. Y-SH, J-XC, and W-JY carried out the experiments. Y-SH and J-XC operated software and visualized the data. Z-BL, JC, W-JY, HH, J-XC, Y-SH, L-LW, and T-TJ collected participant's plasma samples and sorted out clinical information. J-CL, Y-SH, and J-XC integrated the experimental data and fitted classification model. J-CL and Y-SH wrote and revised the manuscript. All authors had checked and approved the manuscript.

ACKNOWLEDGMENTS

We sincerely acknowledge all the participants taking part in this research and especially thank for the assistance from Hong-Bin Zhou at the Zhejiang People's Hospital and Zhi-Wen Pan at Zhejiang Cancer Hospital for collecting blood samples.

DECLARATION OF CONFLICTING INTERESTS

The author(s) declared no potential conflicts of interest with respect to the research, authorship, and/or publication of this article.

ETHICAL APPROVAL

The whole procedure of this study was in accordance with the Ethics Committee of Zhejiang University (China) (approval number 2017023) and was strictly carried out under the standards of Declaration of Helsinki. Informed consent of the subjects was obtained prior to study.

FUNDING

The author(s) disclosed receipt of the following financial support for the research, authorship, and/or publication of this article: This work was supported by grants from National Natural Science Foundation of China (grant number 81772266), Youth Science and Technology Project of Shaoxing Health Commission of China (grant number 2017QN007), Natural Science Foundation of Guangdong Province (grant number 2017A030311014), and Guangzhou Science and Technology Project (grant number 201804010369).

ORCID iDs

Yu-Shuai Han https://orcid.org/0000-0003-1910-3213
Huai Huang https://orcid.org/0000-0002-8978-7043
Ji-Cheng Li https://orcid.org/0000-0002-9631-8931

SUPPLEMENTAL MATERIAL

Supplemental material for this article is available online.

REFERENCES

1. World Health Organization. *Global tuberculosis report 2019*, http://www.who.int/tb/publications/global_report/en/ (2019, accessed 17 October 2019).
2. Hunter RL. Tuberculosis as a three-act play: a new paradigm for the pathogenesis of pulmonary tuberculosis. *Tuberculosis (Edinb)* 2016;**97**:8–17
3. Riaz SM, Bjune GA, Wiker HG, Sviland L, Mustafa T. Mycobacterial antigens accumulation in foamy macrophages in murine pulmonary tuberculosis lesions: association with necrosis and making of cavities. *Scand J Immunol* 2020;**91**:e12866
4. Belay M, Legesse M, Mihret A, Bekele Y, Bjune G, Abebe F. Lipoarabinomannan-specific TNF-α and IFN-γ as markers of protective immunity against tuberculosis: a cohort study in an endemic setting. *APMIS* 2015;**123**:851–7
5. Kim M, Wainwright HC, Locketz M, Bekker L, Walther GB, Dittrich C, Visser A, Wang W, Hsu F, Wiehart U, Tsenova L, Kaplan G, Russell DG. Caseation of human tuberculosis granulomas correlates with elevated host lipid metabolism. *EMBO Mol Med* 2010;**2**:258–74
6. Geng YJ, Hansson GK. Interferon-gamma inhibits scavenger receptor expression and foam cell formation in human monocyte-derived macrophages. *J Clin Invest* 1992;**89**:1322–30
7. Côtes K, Bakala N'Goma JC, Dhouib R, Douchet I, Maurin D, Carrière F, Canaan S. Lipolytic enzymes in Mycobacterium tuberculosis. *Appl Microbiol Biot* 2008;**78**:741–9
8. Tu HH, Yang S, Jiang TT, Wei LL, Shi LY, Liu CM, Wang C, Huang H, Hu YT, Chen ZL, Chen J, Li ZJ, Li JC. Elevated pulmonary tuberculosis biomarker miR-423-5p plays critical role in the occurrence of active TB by inhibiting autophagosome-lysosome fusion. *Emerg Microbes Infect* 2019;**8**:448–60
9. Jiang TT, Shi LY, Wei LL, Li X, Yang S, Wang C, Liu CM, Chen ZL, Tu HH, Li ZJ, Li JC. Serum amyloid A, protein Z, and C4b-binding protein β chain as new potential biomarkers for pulmonary tuberculosis. *PLoS One* 2017;**12**:e173304
10. Yi WJ, Han YS, Wei LL, Shi LY, Huang H, Jiang TT, Li ZB, Chen J, Hu YT, Tu HH, Li JC. l-Histidine, arachidonic acid, biliverdin, and l-cysteine-glutathione disulfide as potential biomarkers for cured pulmonary tuberculosis. *Biomed Pharmacother* 2019;**116**:108980
11. Kastner J, Hossain R, White CS. Epidemiology of lung cancer. *Semin Roentgenol* 2020;**55**:23–40
12. Berry MPR, Graham CM, McNab FW, Xu Z, Bloch SAA, Oni T, Wilkinson KA, Banchereau R, Skinner J, Wilkinson RJ, Quinn C, Blankenship D, Dhawan R, Cush JJ, Mejias A, Ramilo O, Kon OM, Pascual V, Banchereau J, Chaussabel D, O'Garra A. An interferon-inducible neutrophil-driven blood transcriptional signature in human tuberculosis. *Nature* 2010;**466**:973–7
13. Li ZB, Han YS, Wei LL, Shi LY, Yi WJ, Chen J, Huang H, Jiang TT, Li JC. Screening and identification of plasma lncRNAs uc.48+ and NR_105053 as potential novel biomarkers for cured pulmonary tuberculosis. *Int J Infect Dis* 2020;**92**:141–50
14. Scriba TJ, Penn-Nicholson A, Shankar S, Hraha T, Thompson EG, Sterling D, Nemes E, Darboe F, Suliman S, Amon LM, Mahomed H, Erasmus M, Whatney W, Johnson JL, Boom WH, Hatherill M, Valvo J, De Groote MA, Ochsner UA, Aderem A, Hanekom WA, Zak DE, Other Members of the ACS Cohort Study Team. Sequential inflammatory processes define human progression from *M. tuberculosis* infection to tuberculosis disease. *PLoS Pathog* 2017;**13**:e1006687
15. Chegou NN, Heyckendorf J, Walzl G, Lange C, Ruhwald M. Beyond the IFN-γ horizon: biomarkers for immunodiagnosis of infection with Mycobacterium tuberculosis. *Eur Respir J* 2014;**43**:1472–86
16. Du Preez I, Loots DT. New sputum metabolite markers implicating adaptations of the host to Mycobacterium tuberculosis, and vice versa. *Tuberculosis (Edinb)* 2013;**93**:330–7
17. Hadizadeh Tasbiti A, Yari S, Siadat SD, Tabarsi P, Saeedfar K, Yari F. Cellular immune response in MDR-TB patients to different protein expression of MDR and susceptible Mycobacterium tuberculosis: Rv0147, a novel MDR-TB biomarker. *Immunol Res* 2018;**66**:59–66
18. Rockwood N, Du Bruyn E, Morris T, Wilkinson RJ. Assessment of treatment response in tuberculosis. *Expert Rev Resp Med* 2016;**10**:643–54
19. Furse S, de Kroon AIPM. Phosphatidylcholine's functions beyond that of a membrane brick. *Mol Membr Biol* 2015;**32**:117–9
20. Agassandian M, Mallampalli RK. Surfactant phospholipid metabolism. *Biochim Biophys Acta* 2013;**1831**:612–25
21. Rameshwaram NR, Singh P, Ghosh S, Mukhopadhyay S. Lipid metabolism and intracellular bacterial virulence: key to next-generation therapeutics. *Future Microbiol* 2018;**13**:1301–28
22. Aloulou A, Rahier R, Arhab Y, Noiriel A, Abousalham A. Phospholipases: an overview. *Methods Mol Biol* 2018;**1835**:69–105
23. Schmiel DH, Miller VL. Bacterial phospholipases and pathogenesis. *Microbes Infect* 1999;**1**:1103–12
24. Pszenny V, Ehrenman K, Romano JD, Kennard A, Schultz A, Roos DS, Grigg ME, Carruthers VB, Coppens I. A lipolytic lecithin: cholesterol acyltransferase secreted by toxoplasma facilitates parasite replication and egress. *J Biol Chem* 2016;**291**:3725–46
25. De Groote MA, Sterling DG, Hraha T, Russell TM, Green LS, Wall K, Kraemer S, Ostroff R, Janjic N, Ochsner UA. Discovery and validation of a six-marker serum protein signature for the diagnosis of active pulmonary tuberculosis. *J Clin Microbiol* 2017;**55**:3057–71
26. Norum KR. The function of lecithin: cholesterol acyltransferase (LCAT). *Scand J Clin Lab Invest* 2017;**77**:235–6
27. Jamwal SV, Mehrotra P, Singh A, Siddiqui Z, Basu A, Rao KVS. Mycobacterial escape from macrophage phagosomes to the cytoplasm represents an alternate adaptation mechanism. *Sci Rep* 2016;**6**:23089
28. Speer A, Sun J, Danilchanka O, Meikle V, Rowland JL, Walter K, Buck BR, Pavlenok M, Holscher C, Ehrt S, Niederweis M. Surface hydrolysis of sphingomyelin by the outer membrane protein Rv0888 supports

replication of Mycobacterium tuberculosis in macrophages. *Mol Microbiol* 2015;**97**:881–97
29. Goins CM, Schreidah CM, Dajnowicz S, Ronning DR. Structural basis for lipid binding and mechanism of the Mycobacterium tuberculosis Rv3802 phospholipase. *J Biol Chem* 2018;**293**:1363–72
30. Santucci P, Point V, Poncin I, Guy A, Crauste C, Serveau-Avesque C, Galano JM, Spilling CD, Cavalier J, Canaan S. LipG a bifunctional phospholipase/thioesterase involved in mycobacterial envelope remodeling. *Biosci Rep* 2018;**38**:R20181953
31. Kroon PA, Krieger M. The mobility of cholesteryl esters in native and reconstituted low density lipoprotein as monitored by nuclear magnetic resonance spectroscopy. *J Biol Chem* 1981;**256**:5340–4
32. Kondo E, Kanai K. Accumulation of cholesterol esters in macrophages incubated with mycobacteria in vitro. *Jpn J Med Sci Biol* 1976;**29**:123–37
33. Roingeard P, Melo RCN. Lipid droplet hijacking by intracellular pathogens. *Cell Microbiol* 2017;**19**:e12688
34. Libbing CL, McDevitt AR, Azcueta RP, Ahila A, Mulye M. Lipid droplets: a significant but understudied contributor of host-bacterial interactions. *Cells* 2019;**8**:354
35. Yvan-Charvet L, Bonacina F, Guinamard RR, Norata GD. Immunometabolic function of cholesterol in cardiovascular disease and beyond. *Cardiovasc Res* 2019;**115**:1393–407
36. Lu R, Schmitz W, Sampson NS. α-Methyl acyl CoA racemase provides Mycobacterium tuberculosis catabolic access to cholesterol esters. *Biochemistry* 2015;**54**:5669–72
37. Steinmetz A, Hocke G, Saïle R, Puchois P, Fruchart JC. Influence of serum amyloid a on cholesterol esterification in human plasma. *Biochim Biophys Acta* 1989;**1006**:173–8
38. Panousis CG, Zuckerman SH. Regulation of cholesterol distribution in macrophage-derived foam cells by interferon-gamma. *J Lipid Res* 2000;**41**:75–83
39. Guerra-De-Blas PDC, Torres-González P, Bobadilla-Del-Valle M, Sada-Ovalle I, Ponce-De-León-Garduño A, Sifuentes-Osornio J. Potential effect of statins on Mycobacterium tuberculosis infection. *J Immunol Res* 2018;**2018**:7617023
40. Benjamini Y, Hochberg Y. Controlling the false discovery rate: a practical and powerful approach to multiple testing. *J R Stat Soc Series B Stat Methodol* 1995;**57**:289–300

(Received July 15, 2020, Accepted September 23, 2020)